Deuterium isotope effect on the intramolecular electron transfer in *Pseudomonas aeruginosa* azurin

Ole Farver*, Jingdong Zhang†, Qijin Chi†, Israel Pecht‡§, and Jens Ulstrup†

*Institute of Analytical and Pharmaceutical Chemistry, The Royal Danish School of Pharmacy, DK-2100 Copenhagen Ø, Denmark; †Institute of Chemistry, The Technical University of Denmark, DK-2800 Lyngby, Denmark; and ‡Institute of Immunology, The Weizmann Institute of Science, Rehovot 76100, Israel

Communicated by Joshua Jortner, Tel Aviv University, Tel Aviv, Israel, January 26, 2001 (received for review November 3, 2000)

Intramolecular electron transfer in azurin in water and deuterium oxide has been studied over a broad temperature range. The kinetic deuterium isotope effect, k_H/k_D, is *smaller* than unity (0.7 at 298 K), primarily caused by the different activation entropies in water (-56.5 J K^{-1} mol^{-1}) and in deuterium oxide (-35.7 J K^{-1} mol^{-1}). This difference suggests a role for distinct protein solvation in the two media, which is supported by the results of voltammetric measurements: the reduction potential ($E^{0'}$) of $Cu^{2+/+}$ at 298 K is 10 mV more positive in D_2O than in H_2O. The temperature dependence of $E^{0'}$ is also different, yielding entropy changes of -57 J K^{-1} mol^{-1} in water and -84 J K^{-1} mol^{-1} in deuterium oxide. The driving force difference of 10 mV is in keeping with the kinetic isotope effect, but the contribution to $\Delta S^{\ddagger}$ from the temperature dependence of $E^{0'}$ is *positive* rather than negative. Isotope effects are, however, also inherent in the nuclear reorganization Gibbs free energy and in the tunneling factor for the electron transfer process. A slightly larger thermal protein expansion in H_2O than in D_2O (0.001 nm K^{-1}) is sufficient both to account for the activation entropy difference and to compensate for the different temperature dependencies of $E^{0'}$. Thus, differences in driving force and thermal expansion appear as the most straightforward rationale for the observed isotope effect.

Kinetic deuterium or tritium isotope effects (KIE) have long been recognized to reflect crucial mechanistic features in proton and hydrogen atom transfer processes (see, for example, refs. 1–6). KIE were also introduced early as a mechanistically diagnostic tool in hydrolytic metalloenzyme catalysis (7–8). Studies of KIE in metalloenzyme catalysis during the last decade have incorporated increasingly detailed theoretical notions (7–11), for example: proton/deuteron tunneling and multiphonon environmental vibrational excitation (4–6, 12–16); gated proton/deuteron transfer (6, 12–14); proton/deuteron transfer and shallow barriers (17–20); coupled multiproton transfer (17, 21); and stochastic molecular (13–15) and bulk environmental control (12, 22).

Theoretical frames for proton tunneling and KIE are most straightforward when the barriers for proton transfer are high, yielding large values of the KIE ($\gg$1), measured as the ratio between the rate constant for proton and deuteron (or triton) transfer. Proton/deuteron tunneling is here strongly conspicuous. This partially adiabatic limit (4, 6), applies particularly to proton or hydrogen atom transfer between C-donor or -acceptor atoms. Proton transfer between O- and N-donor or -acceptor atoms mostly displays small values (KIE = 1–2.5), reflecting strong hydrogen bond interactions, facile mutual approach between the donor and acceptor groups, and shallow barriers. These barriers correspond to the fully adiabatic limit (4), where the dominating effect of the KIE is reflected in isotope-dependent splitting in the crossing region of the appropriate potential surfaces (6).

In hydrolytic and electron-proton transfer metalloprotein reactions, isotope substitution is, moreover, frequently effected by substitution of H_2O with D_2O solvent. The observation that KIE are frequently small therefore raises the issue of isotope-dependent solvation effects on the thermodynamic and kinetic parameters for electron or proton transfer in metalloproteins. Although bulk dielectric properties of H_2O and D_2O are very similar (23, 24), structural and dynamic details of their solvent properties can, however, be different. The freezing and boiling points are, for example, higher for D_2O than for H_2O; so are the temperatures of density maxima (25, 26). Small differences in protein solvation in H_2O and D_2O can thus be expected and are supported by protein thermal stability differences in the two solvents (27).

We have addressed solvation-based isotope features of protein charge transfer by studying the deuterium isotope effects in a pure intramolecular electron transfer (ET) process of a redox metalloprotein over wide temperature range. The protein is the blue single-copper protein azurin (*Pseudomonas aeruginosa*), which has become a useful model in studies of intramolecular long-range ET in proteins (28). Three-dimensional structures have been determined for a large number of wild-type and single-site mutated azurins (29–34). All are rigid β-sheet proteins containing two redox centers: the copper ion coordinated directly to amino acid residues and a disulfide bridge (RSSR) at the opposite end of the barrel-shaped molecule. We have previously demonstrated that long-range ET between these two centers can be induced after pulse radiolytic single-electron reduction of RSSR (35–41). We examined the effects of specific structural changes on the rate of intramolecular ET between the $RSSR^-$ radical and the Cu(II) center by using wild-type and single-mutant azurins. In the present study, the solvent-based deuterium isotope effects on intramolecular ET between $RSSR^-$ and the Cu(II) center have been pursued. Results show a kinetic deuterium isotope effect that is, intriguingly, *smaller* than unity. This feature is caused by a significantly more negative apparent activation entropy for the reaction in H_2O than in D_2O, a result that clearly excludes that proton or hydrogen atom tunneling is significant. The oxidation potential of the copper center is found to be 10 mV more positive in D_2O than in H_2O, in keeping with the observed ''inverse'' KIE. The sign of the difference between the formal entropies (temperature coefficients) in the two solvents is, however, opposite to that required for accordance with the kinetic data. Other parameters must therefore be invoked, and a slightly stronger thermal expansion of the protein in H_2O than in D_2O presently appears as the simplest one.

Materials and Methods

Proteins. *P. aeruginosa* azurin was isolated as described earlier (36). Protein solutions in D_2O (99.9%; Cambridge Isotope Laboratories, Cambridge, MA) were prepared by repeatedly concentrating buffered azurin solutions in Centricon-10 (Amicon) units. The buffer was 10 mM phosphate at pH 7.0. Deuterated buffer solutions were produced by neutralizing

Abbreviations: ET, electron transfer; KIE, kinetic isotope effects.

§To whom reprint requests should be addressed. E-mail: israel.pecht@weizmann.ac.il.

The publication costs of this article were defrayed in part by page charge payment. This article must therefore be hereby marked "*advertisement*" in accordance with 18 U.S.C. §1734 solely to indicate this fact.

www.pnas.org/cgi/doi/10.1073/pnas.071043798

D_3PO_4 (Sigma, 99% D) solutions, with 0.1 M in NaOD in D_2O. Measured pH values in D_2O were not corrected for isotope effects.

Solutions of 0.1 M in sodium formate and 10 mM in phosphate were deaerated and saturated with N_2O by continuous bubbling in glass syringes. After adjustment of pH to 7.0, the concentrated azurin solution was added. N_2O bubbling was continued for another 5 min, and the solution was then transferred anaerobically into the pulse radiolysis cuvette.

Kinetic Measurements. Pulse radiolysis experiments were carried out on a Varian V-7715 linear accelerator at the Hebrew University in Jerusalem. Electrons accelerated to 5 MeV were used with pulse lengths in the range 0.1–1.5 μs, equivalent to 0.6–10 μM of CO_2^- radical ions. All measurements were carried out anaerobically, under purified argon at a pressure slightly in excess of 1 atm (1 atm = 101.3 Pa) in a $4 \times 2 \times 1$ cm^3 Spectrosil (Helma, Müllheim, Germany) cuvette. Three light passes were used, which resulted in an overall optical path length of 12.3 cm. A 150-W xenon lamp produced the analyzing light beam, and optical filters with cutoff at 385 nm were used to avoid photochemistry and light scattering. The data acquisition system consisted of a Tektronix 390 A/D transient recorder connected to a personal computer. In each experiment, 2,000 data points were collected, divided equally between two different time scales. Usually the processes were followed over at least three half lives. Each kinetic run was repeated at least four times. The data were fitted to a sum of exponentials by using a nonlinear least-squares program written in MATLAB (Mathworks, Natick, MA). The temperature of the reaction solutions was controlled by a thermostating system and continuously monitored by a thermocouple attached to the cuvette. Almost all reactions were performed under pseudo-first-order conditions, with typically a 10-fold excess of oxidized protein over reductant.

Electrochemistry. The same azurin and buffer solutions in H_2O and D_2O were used as for the kinetic data. Millipore (Milli-Q Housing, 18.2 MΩ) water was used for the solutions using H_2O solvent. All glassware and other utensils were cleaned as previously mentioned (42). Glassware for D_2O was dried after cleaning in Millipore water and rinsed by D_2O before use.

An in-house-built nonisothermal cell was used for electrochemical measurements. A saturated calomel electrode kept at room temperature was mounted into a 120-mm salt bridge isolated from the thermostated electrochemical cell. Edge-plane pyrolytic graphite served as working electrodes (WEs) and a platinum wire put close to WE as counter electrode. The temperature of the solutions was controlled ($\pm$0.1°C) in the range 4–46°C by a constant temperature bath/circulator (Neslab, Portsmouth, NH) and monitored by a thermometer (Manofix Manometer, Frode Pedersen, Allerød, Denmark). Temperature accuracy of the cell was 0.1°C.

All electrochemical experiments were carried out by using an Eco Chemie Autolab, Utrecht, the Netherlands, potentiostat controlled by the general-purpose electrochemical system software. Purified Ar (Chrompack, 5 N, Varian) was applied to deoxygenate all solutions. An argon stream over the solution was maintained during the measurements. Before use, the edge-plane pyrolitic graphite was polished to a mirror-like state successively by a 1 μm and 0.05 μm Al_2O_3 slurry, then washed by water, followed by supersonication twice in water or D_2O.

Formal potentials were determined from reversible cyclic voltammograms recorded at low scan rate (10 mV/s). The data shown are average values of four independent experiments from two edge-plane pyrolitic graphite electrodes. All electrode potentials are referred to the standard hydrogen electrode.

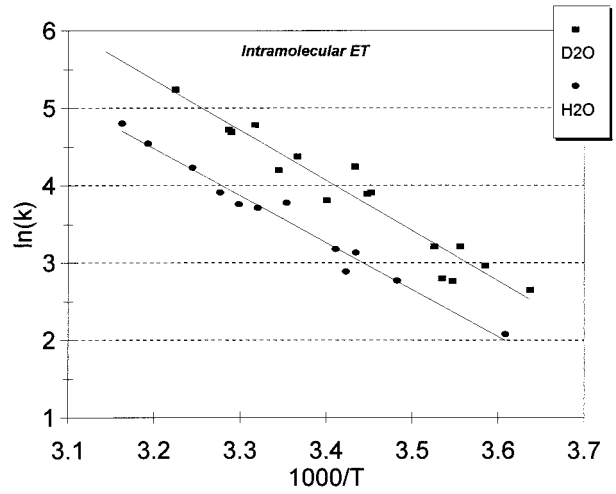

Fig. 1. Temperature dependence of intramolecular $RSSR^-$ to Cu^{2+} ET in azurin. ●, in H_2O; ■, in D_2O.

Results

Kinetic Measurements. Pulse radiolytically produced CO_2^- radicals reduce both the copper(II) site and the disulfide bridge in azurin at essentially diffusion-controlled rates (35–41). The Cu(II)→Cu(I) reduction results in an absorption decrease at 625 nm, while the $RSSR^-$ radicals formed absorb strongly around 410 nm. After these two bimolecular reactions, *i* and *ii* below, the $RSSR^-$ absorption was found to decay concomitantly with further decrease in the characteristic Cu(II) absorption (the slow phase, *iii*).

$$\text{RSSR-Az[Cu(II)]} + CO_2^- \rightarrow \text{RSSR-Az[Cu(I)]} + CO_2, \quad \textbf{[i]}$$

$$\text{RSSR-Az[Cu(II)]} + CO_2^- \rightarrow \text{RSSR}^-\text{-Az[Cu(II)]} + CO_2, \quad \textbf{[ii]}$$

$$\text{RSSR}^-\text{-Az[Cu(II)]} \rightarrow \text{RSSR-Az[Cu(I)]}. \quad \textbf{[iii]}$$

The rate of reaction *iii* was independent of protein concentration between 1 and 10 μM and is thus an intramolecular process. At pH 7.0 and 298 K, the rate constant for *intra*molecular ET in *P. aeruginosa* azurin in H_2O is 44 ± 7 s^{-1}, in agreement with earlier results (35). The process becomes significantly faster in D_2O (66 ± 10 s^{-1}). The reactions were studied over a temperature range from 274 K to 317 K (Fig. 1). The results, including activation parameters, are summarized in Table 1.

It is obvious from Fig. 1 and Table 1 that the different rates in the two media are caused by an apparent entropy effect. This entropy effect which excludes significant contributions from proton or hydrogen atom transfer as well as proton tunneling as a likely cause for the kinetic deuterium isotope effect. A

Table 1. Kinetic and thermodynamic parameters; pH 7.0 and 298 K

Parameter	H_2O	D_2O
k_{298}/s^{-1}	44 ± 7	66 ± 10
$\Delta H^{\neq}$/kJ mol^{-1}	47.5 ± 2.2	51.5 ± 3.7
$\Delta S^{\neq}$/J K^{-1} mol^{-1}	-56.5 ± 3.5	-35.7 ± 2.5
$E^{0'}_{298}$/mV	306 ± 1	316 ± 1
ΔH^0/kJ mol^{-1}	-46.7 ± 1.2	-55.8 ± 2.5
ΔS^0/J K^{-1} mol^{-1}	-56.9 ± 1.4	-84.4 ± 3.7

ΔH^0 and ΔS^0 are the formal enthalpy and entropy of the $Cu^{2+/+}$ reduction potential, $E^{0'}_{Cu}$, determined as in Eq. **3**. $E^{0'}_{298}$ is the value at 25°C.

BIOPHYSICS

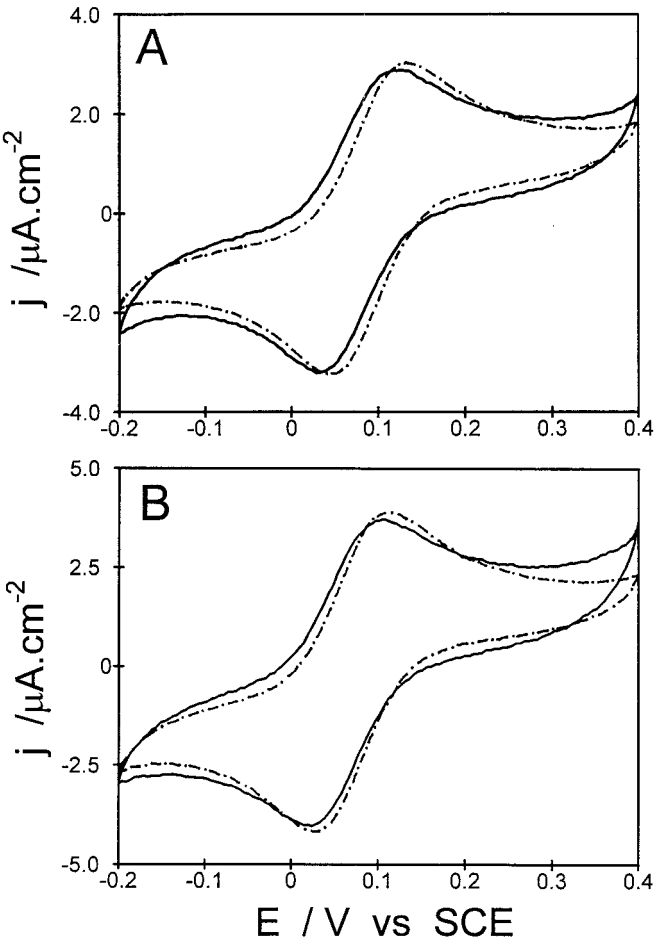

Fig. 2. Cyclic voltammograms at bare EPG in 0.3 mM azurin, 10 mM phosphate buffer, and 100 mM formate (pH 7.0). Scan rate, 10 mV/s. Dashed line, in D_2O. Solid line, in H_2O. (*A*) 4.6°C; (*B*) 24.7°C.

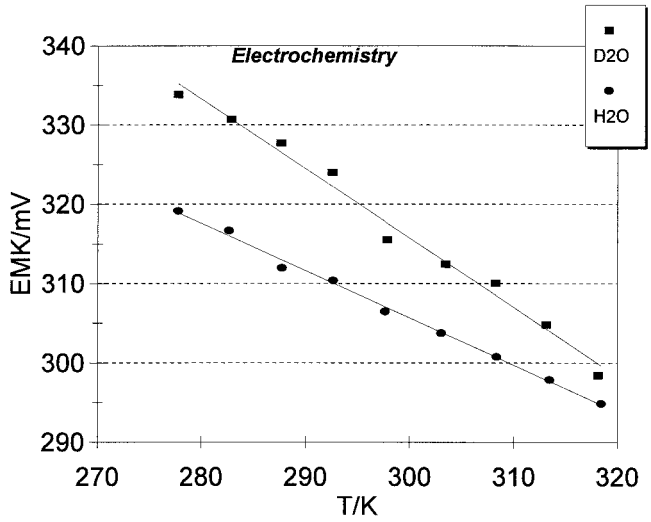

Fig. 3. $E^{0'}$ for Cu^{2+}/Cu^{+} at varying temperatures. Potentials are given relative to a Standard Hydrogen Electrode. ●, in H_2O; ■, in D_2O.

rationale for the observed values of the smaller than unity KIE would thus require large changes in vibrational frequencies (such as in dissociative proton transfer) or other effects that are not easily reconciled with the chemical properties of the ET system in *i–iii*. Causes rooted in different solvation in H_2O and D_2O can, however, be addressed with a view to the following broadly used frame for ET processes (12):

$$k = \kappa_{el}\frac{\omega_{eff}}{2\pi}\exp\left[-\frac{(\lambda_s + \Delta G^0)^2}{4\lambda_s k_B T}\right]. \qquad [1]$$

λ_s in Eq. **1** is the solvent reorganization Gibbs free energy, ΔG^0 the reaction Gibbs free energy or driving force, ω_{eff} the effective frequency of all the nuclear modes reorganized, and κ_{el} the electronic transmission coefficient. k_B is Boltzmann's constant and T the temperature.

Isotope effects are in principle associated with *all* the quantities in Eq. **1**. ω_{eff} is expected to exhibit "normal" behavior, i.e., to be larger for H_2O than for D_2O. λ_s is not directly experimentally accessible (see, however, below). Structureless dielectric models for λ_s (43–45) would give insignificant values of the isotope effect, as the dielectric permitivities for the two media are very similar (23, 24). Models that incorporate solvent structural features such as nonlocal dielectric features (46) would give a KIE if, for example, the inertial polarization correlation length and the temperature coefficient of this quantity depend on the isotope. Such an effect is likely, but independent experimental verification is elusive. κ_{el} could, however, be expected to depend on the temperature. In the simplest sense, thermal expansion of the protein would give a lower value of κ_{el}, as the temperature increases because of increasing average distance between the two redox centers. This effect could also be different in H_2O and D_2O. The effect is conceptually straightforward and could in principle be probed by molecular dynamics simulations. Only a very slightly solvent isotope sensitive thermal expansion is in fact enough to cause KIEs in keeping with those observed. The driving force, ΔG^0, is then left as the quantity in Eq. **1** most directly accessible experimentally.

Electrochemistry. The driving force, ΔG^0, can be addressed by

$$\Delta G^{0'} = -eF(E^{0'}_{Cu} - E^{0'}_{RSSR}) \qquad [2]$$

where $E^{0'}_{Cu}$ and $E^{0'}_{RSSR}$ are the formal oxidation potentials of the copper center and the disulfide bridge, respectively, e the electronic charge, and F Faraday's number. $E^{0'}_{Cu}$ in H_2O and D_2O can be determined by cyclic voltammetry, which requires, however, great care as the differences between the two media are small. $E^{0'}_{RSSR}$ cannot be determined in this way. The value broadly used originates from the midpoint potential of a mixed disulfide derivative formed between a protein-bound sulfhydryl and 5,5′-dithiobis(2-nitrobenzoic acid) (47). Attention was therefore given to $E^{0'}_{Cu}$ and the deuterium isotope effect on this quantity.

Fig. 2 shows a representative cyclic voltammogram of the $Cu^{2+/+}$ center of azurin at 4.6°C (*A*) and 24.7°C (*B*). The midpoint potential difference between H_2O and D_2O is small but shows clearly a higher value for D_2O ($E^{0'D}_{Cu}$ = 316 mV, 298 K) than for H_2O ($E^{0'H}_{Cu}$ = 306 mV, 298 K). Fig. 3 shows the temperature variation of $E^{0'D}_{Cu}$ and $E^{0'H}_{Cu}$ in the range 4.6–45.0°C. The data for H_2O closely follow those in previous reports (48, 49). The temperature variation for D_2O is significantly stronger which testifies clearly to different solvation patterns in the two media and to conspicuous solvation contributions to the KIE. It is shown in the next section that this effect alone cannot explain the observed kinetic pattern. The oxidation potential variation with the temperature is thermally reversible for H_2O, whereas the midpoint potential is slightly (≈7–8 mV at 24.7°C) shifted towards negative values after a temperature cycle in D_2O. The apparent formal enthalpy and entropy values were calculated from the data in Fig. 3 by the relations

$$\Delta G^{0I}_{\mathrm{Cu}} = -eFE^{0I}_{\mathrm{Cu}}, \quad \Delta S^{0I}_{\mathrm{Cu}} = eF\frac{dE^{0I}_{\mathrm{Cu}}}{dT}$$

$$\Delta H^{0I}_{\mathrm{Cu}} = -eFE^{0I}_{\mathrm{Cu}} + eFT\frac{dE^{0I}_{\mathrm{Cu}}}{dT}; I = \mathrm{H, D}, \qquad [3]$$

and are shown in Table 1. In the following section, we shall focus on the differences between these quantities in H_2O and D_2O.

Discussion

The kinetic data show, notably, that the KIE for the intramolecular ET reaction in azurin (*iii*) is

$$\frac{k_{\mathrm{H}}}{k_{\mathrm{D}}} = 0.67 \pm 0.21,$$

i.e., smaller than unity. k_{H} and k_{D} are the rate constants of reaction *iii* in H_2O and D_2O, respectively. As noted, such a ratio excludes proton/deuteron tunneling as the primary cause for the observed effect, in keeping with the nature of reaction *iii* as a pure ET process. The voltammetric data also point to marked differences in both the oxidation potential of the copper center and in its temperature coefficient in the two solvents. These observations strongly suggest that solvation and protein dynamic effects are causes of the KIE.

The isotope effects can be illuminated by the following consideration. Disregarding at first isotope effects on the transmission coefficient, we can recast Eq. **1** in terms of the chemical transfer coefficient (12), α:

$$k \propto \exp\left[-\frac{\alpha(1-\alpha)\lambda_s}{k_{\mathrm{B}}T} - \frac{\alpha\Delta G^0}{k_{\mathrm{B}}T}\right]; \quad \alpha = -k_{\mathrm{B}}T\frac{d\ln k}{d\Delta G^0}. \qquad [4]$$

ΔG^0 for reaction *iii* has been determined to be -0.7 eV in *P. aeruginosa* azurin (35). λ_s cannot be determined directly (see, however, below), but free energy relations of other redox metalloproteins (50–52) and theoretical models based on dielectric continuum theory (43–45) or force field calculations (53) suggest values of about 1.0 eV. Introducing these numbers in Eq. **4** gives $\alpha = 0.15$, which will be used in the following. If λ_s is smaller, α is also smaller. The process would then approach the activationless free energy range, and the following analysis would need modifications.

Focusing on ΔG^0, the ratio between the rate constants in H_2O and D_2O can be given the form

$$\frac{k_{\mathrm{H}}}{h_{\mathrm{D}}} \approx \exp\left[-\frac{\alpha(\Delta G^0_{\mathrm{H}} - \Delta G^0_{\mathrm{D}})}{k_{\mathrm{B}}T}\right] = \exp\left[-\frac{\alpha(\Delta H^0_{\mathrm{H}} - \Delta H^0_{\mathrm{D}})}{k_{\mathrm{B}}T}\right]\exp\left[\frac{\alpha(\Delta S^0_{\mathrm{H}} - \Delta S^0_{\mathrm{D}})}{k_{\mathrm{B}}}\right], \qquad [5]$$

where the formal reaction enthalpies and entropies have been introduced. The subscripts H and D refer to H_2O and D_2O, respectively. We ascribe, further, all isotope and temperature variation solely to the copper center primarily because of the lack of data for the disulfide group, but warranted by the smaller electrostatic charges of the $RSSR/RSSR^-$ couple. A more precise analysis could be reconsidered when appropriate data are available.

With the following definitions:

$$\Delta(\Delta H^0) = \Delta H^0_{\mathrm{H}} - \Delta H^0_{\mathrm{D}}, \quad \Delta(\Delta S^0) = \Delta S^0_{\mathrm{H}} - \Delta S^0_{\mathrm{D}};$$

$$\Delta(\Delta G^0) = \Delta G^0_{\mathrm{H}} - \Delta G^0_{\mathrm{D}}; \qquad [6]$$

we now can write:

$$\frac{\Delta(\Delta G^0)}{eF} = -\Delta(\Delta E^{0\prime}) = -(E^{0\prime\mathrm{H}}_{\mathrm{Cu}} - E^{0\prime\mathrm{H}}_{\mathrm{SS}}) + (E^{0\prime\mathrm{D}}_{\mathrm{Cu}} - E^{0\prime\mathrm{D}}_{\mathrm{SS}}) \qquad [7]$$

$$\approx -\Delta E^{0\prime}_{\mathrm{HD}} = \Delta E^{0\prime\mathrm{H}}_{\mathrm{Cu}} - \Delta E^{0\prime D}_{Cu}$$

$$\frac{\Delta(\Delta S^0)}{eF} = -\frac{d\Delta(\Delta G^0)}{eFdT} \approx \frac{d\Delta E^{0\prime}_{\mathrm{HD}}}{dT} \qquad [8]$$

$$\Delta(\Delta \mathrm{H}^0) = \Delta(\Delta G^0) + T\Delta(\Delta S^0) = -eF\Delta E^{0\prime}_{\mathrm{HD}} + eFT\frac{d\Delta E^{0\prime}_{\mathrm{HD}}}{dT}. \qquad [9]$$

From the thermodynamic data in Table 1, we find: $\Delta(\Delta G^0) = +1.0$ kJ mol^{-1} (0.010 eV); $\Delta(\Delta \mathrm{H}^0) = +9.1$ kJ mol^{-1} and $\Delta(\Delta S^0) = +27.5$ J K^{-1} mol^{-1}. Thus, from Eq. **5**

$$\frac{k_{\mathrm{H}}}{k_{\mathrm{D}}}(25°\mathrm{C}) = \exp\left[-\frac{0.15 \times 0.010}{k_{\mathrm{B}}T}\right] = 0.9. \qquad [10]$$

This is close enough to the observed ratio of 0.7. Further,

$$\Delta H^{\neq}_{\mathrm{H}} - \Delta H^{\neq}_{\mathrm{D}} \approx \alpha \times \Delta(\Delta H^0) = 1.4 \text{ kJ mol}^{-1}.$$

Such a small value accords with the small experimentally determined difference of -4.0 kJ mol^{-1}.

However,

$$\Delta S^{\neq}_{\mathrm{H}} - \Delta S^{\neq}_{\mathrm{D}} \approx \alpha \times \Delta(\Delta S^0) = 4 \text{ J K}^{-1} \text{ mol}^{-1},$$

which should be compared with the experimentally determined difference: -21 J K^{-1} mol^{-1}, i.e. a difference of 25 J K^{-1} mol^{-1}.

It therefore appears that consideration of other effects is needed. The simplest cause could be the thermal variation of the electronic transmission coefficient, which depends on the distance, R, between electron donor and acceptor approximately as:

$$\kappa_{\mathrm{el}} = \kappa^0_{\mathrm{el}}\exp(-\beta R) \qquad [11]$$

This form can be integrated into Eq. **1** by the following formal contribution to the activation Gibbs free energy in addition to λ_s and ΔG^0.

$$\Delta G^{\neq}_{\mathrm{el}} = -k_{\mathrm{B}}T\ln\left(\frac{\hbar\omega_{\mathrm{eff}}}{k_{\mathrm{B}}T}\right) - k_{\mathrm{B}}T\ln\kappa^0_{\mathrm{el}} + k_{\mathrm{B}}T\beta R(T). \qquad [12]$$

Eq. **12** converts Eq. **1** to a form equivalent to absolute rate theory (54). The corresponding activation entropy becomes

$$\Delta S^{\neq}_{\mathrm{el}} \approx k_{\mathrm{B}}\ln\left(\frac{\hbar\omega_{\mathrm{eff}}}{k_{\mathrm{B}}T}\right) - k_{\mathrm{B}} + k_{\mathrm{B}}\ln\kappa^0_{\mathrm{el}} - k_{\mathrm{B}}\beta R - k_{\mathrm{B}}T\beta\frac{dR}{dT}. \qquad [13]$$

For this contribution to the kinetic deuterium isotope effect, we can write:

$$\Delta S^{\neq}_{\mathrm{el,HD}} \approx -k_{\mathrm{B}}\beta(R_{\mathrm{H}} - R_{\mathrm{D}}) - k_{\mathrm{B}}T\beta\left(\frac{dR_{\mathrm{H}}}{dT} - \frac{dR_{\mathrm{D}}}{dT}\right). \qquad [14]$$

As noted, the difference in activation entropy should compensate for -25 J K^{-1} mol^{-1}, altogether.

The first term in Eq. **12** would give a change in ET distance of 0.3 nm between H_2O and D_2O, which is quite unrealistic. However, by using the second term, a difference in distance dependence of only 0.001 nm/K is required. This value is plausible and means that the protein undergoes a slightly larger thermal expansion in water than in deuterium oxide.

The combined effect of different reduction potentials of the copper center and small differences in thermal expansion of the

protein in the two solvents thus seems to be in keeping with the kinetic and thermodynamic deuterium isotope effects in the simplest possible fashion.

Several other effects could, however, result from thermal expansion of the protein structure. These would be, particularly: changes in both vibrational amplitudes and frequencies of the "bulk" or collective protein modes and increased sensitivity of local mode frequencies and equilibrium configurations around the two ET centers to the electric field changes associated with the ET process. Although the nature of these partly opposite effects can be appreciated, their isotope dependence is, however, much harder to address.

The following additional observations could hold clues to a more complete mapping of the isotope effects. First, perhaps the best probe of the thermal expansion is molecular dynamics simulation of the protein over the appropriate temperature range, but this would require inclusion of large solvent molecular assemblies. Secondly, although the isotope dependence of the environmental reorganization Gibbs free energy, λ_s, is elusive, a recent report of the electrochemical properties of *P. aeruginosa* azurin (55) could hold an experimental clue to this quantity. Azurin can be immobilized hydrophobically in well defined monolayers on single-crystal Au(111) surfaces modified by variable-length alkylthiolates of chain lengths in excess of ≈ 9 CH_2 groups. Current–overvoltage relations (i.e., free energy relations) of azurin in such environments over broad overvoltage ranges approaching the activationless range were achieved, with a resulting determination of λ_s. Such experiments are demanding but could be transferred to D_2O and illuminate, experimentally, kinetic deuterium isotope effects on the environmental reorganization Gibbs free energy. The data and theoretical notions above could, thus, be important broadly for metalloprotein reactivity where small isotope effects are encountered.

O.F. thanks the Danish Natural Science Research Council for financial support. I.P. acknowledges the support of the German–Israeli Foundation and the Volkswagen Foundation. J.U. acknowledges financial support from the Danish Technical Science Research Council.

1. Bell, R. P. (1973) *The Proton in Chemistry* (Chapman & Hall, Oxford).
2. Bell, R. P. (1980) *The Tunnel Effect in Chemistry* (Chapman & Hall, Oxford).
3. Schowen, R. L. (1977) in *Isotope Effects on Enzyme Catalyzed Reactions,* eds. Cleland, W. W., O'Leary, M. H. & Northrup, D. B. (University Park Press, Baltimore), pp. 64–99.
4. Levich, V. G., Dogonadze, R. R., German, E. D., Kuznetsov, A. M. & Kharkats, Yu. I. (1970) *Electrochim. Acta* **15,** 353–367.
5. Benderskij, V. A., Makarov, D. E. & Wight, C. A. (1994) *Chemical Dynamics at Low Temperatures* (Wiley, New York).
6. Kuznetsov, A. M. & Ulstrup, J. (1999) *Can. J. Chem.* **77,** 1085–1096.
7. Kaiser, B. L. & Kaiser, E. T. (1969) *Proc. Natl. Acad. Sci. USA* **64,** 36–41.
8. Silverman, D. N. & Lindskog, S. (1988) *Acc. Chem. Res.* **21,** 30–36.
9. Vidakovic, M., Sligar, S. G., Li, H. & Poulos, T. L. (1998) *Biochemistry* **37,** 9211–9219.
10. Cha, Y., Murray, C. J. & Klinman, J. P. (1989) *Science* **243,** 1325–1330.
11. Kohen, A. & Klinman, J. P. (1998) *Acc. Chem. Res.* **31,** 397–404.
12. Kuznetsov, A. M. & Ulstrup, J. (1999) *Electron Transfer in Chemistry and Biology: An Introduction to the Theory* (Wiley, Chichester, U.K.).
13. Borgis, D. & Hynes, J. T. (1991) *J. Chem. Phys.* **94,** 3619–3628.
14. Borgis, D. & Hynes, J. T. (1996) *J. Phys. Chem.* **100,** 1118–1128.
15. Fang, J.-Y. & Hammes-Schiffer, S. (1997) *J. Chem. Phys.* **106,** 8442–8454.
16. Cukier, R. J. (1994) *J. Phys. Chem.* **98,** 2377–2381.
17. Scheiner, S. (1985) *Acc. Chem. Res.* **18,** 174–180.
18. Kuznetsov, A. M. & Ulstrup, J. (1994) *Chem. Phys.* **188,** 131–141.
19. Warshel, A., Papazyan, A. & Kollman, P. A. (1995) *Science* **269,** 102–103.
20. Cleland, W. W. & Kreevoy, M. M. (1994) *Science* **264,** 1887–1890.
21. Dogonadze, R. R., Ulstrup, J. & Kharkats, Yu. I. (1972) *Dokl. Akad. Nauk SSSR, Ser. Fiz. Khim.* **207,** 640–643.
22. Sumi, H. & Ulstrup, J. (1988) *Biochim. Biophys. Acta* **955,** 26–42.
23. Malmberg, C. G. (1958) *J. Res. Nat. Bur. Stand.* **60,** 609–612.
24. Vidulich, G. A., Evans, D. F. & Kay, R. L. (1967) *J. Phys. Chem.* **71,** 656–662.
25. Eisenberg, D. & Kauzman, W. (1969) *The Structure and Properties of Water* (Clarendon, Oxford).
26. Franks, F. (1983) *Water* (R. Soc. Chem., Cambridge, U.K.).
27. Makhatadze, G. I., Clore, G. M. & Gronenborn, A. M. (1995) *Nat. Struct. Biol.* **2,** 852–855.
28. Farver, O. & Pecht, I. (1999) *Advances in Chemical Physics*, eds. Jortner, J. & Bixon, M. (Wiley, New York), Vol. 107, pp. 555–590.
29. Baker, E. N. (1988) *J. Mol. Biol.* **203,** 1071–1095.
30. Hammann, C., Messerschmidt, A., Huber, R., Nar, H., Gilardi, G. & Canters, G. W. (1996) *J. Mol. Biol.* **255,** 362–366.
31. Nar, H., Messerschmidt, A., Huber, R., van de Kamp, M. & Canters, G. W. (1991) *J. Mol. Biol.* **221,** 765–777.
32. Nar, H., Messerschmidt, A., Huber, R., van de Kamp, M. & Canters, G. W. (1991) *J. Mol. Biol.* **218,** 427–447.
33. Romero, A., Hoitink, C. W., Nar, H., Huber, R., Messerschmidt, A. & Canters, G. W. (1993) *J. Mol. Biol.* **229,** 1007–1021.
34. Messerschmidt, A., Prade, L., Kroes, S. J., Sanders-Loehr, J., Huber, R. & Canters, G. W. (1998) *Proc. Natl. Acad. Sci. USA,* **95,** 3443–3448.
35. Farver, O. & Pecht, I. (1989) *Proc. Natl. Acad. Sci. USA,* **86,** 6968–6972.
36. Farver, O. & Pecht, I. (1992). *J. Am. Chem. Soc.* **114,** 5764–5767.
37. Farver, O., Skov, L. K., van de Kamp, M., Canters, G. W. & Pecht, I. (1992) *Eur. J. Biochem.* **210,** 399–403.
38. Farver, O., Skov, L. K., Pascher, T., Karlsson, B. G., Nordling, M., Lundberg, L. G., Vanngard, T. & Pecht, I. (1993) *Biochemistry* **32,** 7317–7322.
39. Farver, O., Skov, L. K., Gilardi, G., van Pouderoyen, G., Canters, G. W., Wherland, S. & Pecht, I. (1996). *Chem. Phys.* **204,** 271–277.
40. Farver, O., Bonander, N., Skov, L. K. & Pecht, I. (1996) *Inorg. Chim. Acta* **243,** 127–133.
41. Farver, O., Jeuken, L. J. C., Canters, G. W. & Pecht, I. (2000) *Eur. J. Biochem.* **267,** 3123–3129.
42. Zhang, J., Chi, Q., Nielsen, J. U., Friis, E. P., Andersen, J. E. T. & Ulstrup, J. (2000) *J. Langmuir* **16,** 7229–7237.
43. Kharkats, Yu. I. & Kristhalik, L. I. (1985) *J. Theor. Biol.* **112,** 221–241.
44. Kharkats, Yu. I. & Ulstrup, J. (1990) *Chem. Phys.* **141,** 117–129.
45. Kharkats, Yu. I. & Ulstrup, J. (1999) *Chem. Phys. Lett.* **303,** 320–324.
46. Kornyshev, A. A. (1985) in *The Chemical Physics of Solvation: Part A.-Theory of Solvation,* eds. Dogonadze, R. R., Kálmán, E., Kornyshev, A. A. & Ulstrup, J. (Elsevier, Amsterdam), pp. 77–118.
47. Faraggi, M. & Klapper, M. H. (1988) *J. Am. Chem. Soc.* **110,** 5753–5756.
48. Taniguchi, V. T., Sailasuta-Scott, N., Anson, F. C. & Gray, H. B. (1980) *Pure Appl. Chem.* **52,** 2275–2281.
49. Battistuzzi, G., Borsari, M., Loschi, L., Righi, F. & Sola, M. (1999) *J. Am. Chem. Soc.* **121,** 501–506.
50. Winkler, J. R. & Gray, H. B. (1992) *Chem. Rev.* **92,** 369–379.
51. Meyer, T. E., Watkins, J. A., Przysiecki, C. T., Tollin, G. & Cusanovich, M. A. (1984) *Biochemistry* **23,** 4761–4767.
52. Andersen, N. H., Hervás, Navarro, J. A., De la Rosa, M. A. & Ulstrup, J. (1998) *Inorg. Chim. Acta* **272,** 109–114.
53. Warshel, A. (1991) *Computer Modelling of Chemical Reactions in Enzymes and Solutions* (Wiley, New York).
54. German, E. D. (1983) *Rev. Inorg. Chem.* **5,** 123–184.
55. Chi, Q., Zhang, J., Andersen, J. E. T. & Ulstrup, J. (2001) *J. Phys. Chem. B,* in press.